RSC Advances

RSC Advances

www.rsc.org/advances

ROYAL SOCIETY
OF **CHEMISTRY**

www.rsc.org/advances

Synthesis of super-hydrophobic Ni-ITO nanocomposite with pine-cone and spherical shaped micro-nanoarchitectures by pulse electrodeposition and its electrocatalytic application

P. Sivasakthi, G. N. K. Ramesh Bapu*, Maruthai Chandrasekaran and S. S. Sreejakumari

CSIR-Central Electrochemical Research Institute

Karaikudi 630006, Tamil Nadu, India

Abstract

A super-hydrophobic Ni-ITO nanocomposite on mild steel substrate was prepared by pulse electrodeposition method from nickel sulphamate electrolyte and was examined as electrocatalyst for electo-reduction of nitrobenzene. The chemical composition, surface morphology, surface topography, preferred orientation and contact angle of deposited Ni and Ni-ITO nanocomposite electrodes were analysed by EDAX, FE-SEM, AFM, XRD and static contact angle mode using Laplace–Young calculation method. Electrochemical reduction of nitrobenzene on this super-hydrophobic electrode was studied by cyclic voltammetry. The spherical nanostructures with high active surface area, high contact angle (161.8˚) and higher electrocatalytic performance for the reduction of nitrobenzene were obtained on super-hydrophobic Ni-ITO nanocomposite compared to nickel deposit alone (contact angle 110˚).

Introduction

In recent years, multifunctional super-hydrophobic surfaces with two or more functional properties of materials are of interest for fundamental research and in many practical applications. Surfaces with larger contact angle (CA) greater than 150˚ are called super-hydrophobic surfaces.[1-3] Super-hydrophobic surfaces are obtained by creating micro-nano structured hydrophobic surfaces or chemically modifying the micro-nano structured surface with low surface free energy materials or enhancing surface roughness.[4-8] Super-hydrophobic surfaces have been widely used in electrical industry, micro-fluidic devices,

satellite antennas and conductors due to their water repellence, self-cleaning, anti-corrosion, and anti-icing properties.[9-14] Therefore, it is important to develop a facile and low cost method to prepare super-hydrophobic surfaces with multifunctional properties for wide range of practical applications. Super-hydrophobic surfaces can be prepared by various methods such as plasma etching, chemical vapour deposition, anodic oxidation, phase separation, sol-gel method and electrodeposition.[15-21] However, electrodeposition is one of the best method due to its convenience and economy.[22] In electrodeposition, pulse current plating offers a greater control over the structure and properties of electrodeposits than the conventional direct current plating and pulse reverse current plating.[23] Nanocomposite as super-hydrophobic materials find wide application in electrocatalysis and electroanalysis due to their high surface/volume ratio and chemical stability. Hui Zhang et al. reported superhydrophobicity of shape controlled gold nanoarchitectures for electrocatalytic properties.[24] Metals (e.g., Au, Pt, Pd, Cu, Ni and Ag) and metal oxides (e.g., TiO_2 and ITO) nanocomposite materials can be used as electro-catalyst (electro-reduction or electro-oxidation) due to their increased surface area, enhanced mass transport and catalysis.[25-26] Nickel possesses high hardness, better tribological, anticorrosion, antioxidation and hydrophobic properties. Nickel suspensions with nanoparticles provide super-hydrophobicity, which can greatly broaden its application. Corrosion resistance and long-term durability of super-hydrophobic nickel film using ethylenediammonium dichloride as crystal modifier prepared by electrodeposition process were studied by Khorsand et al.[27] Super-hydrophobic nickel films with micro-nano hierarchical structure using ethylenediammonium dichloride as crystal modifier prepared by electrodeposition.[28] Indium tin oxide (ITO) nanoparticles find as useful conducting materials for the fabrication of devices due to mechanical characteristics, low cost, high electrical conductivity, wide electrochemical working window, stability and high surface area.[29] Hoo keun park et al. reported the fabrication and characterization of

large-scale multifunctional transparent ITO nanorod films.[30] Although very few reports have

been published on Ni-ITO nanocomposite electrode as an electrocatalyst for certain analytes,

there has hitherto been no report on the pulse electrodeposited super-hydrophobic Ni-ITO

nanocomposites for the electro-reduction of nitrobenzene. In this article, we present super-

hydrophobic Ni-ITO nanocomposite by pulse electrodeposition for electro-reduction of

nitrobenzene as shown in Scheme 1. Ni-ITO nanocomposite is expected to improve the

technological advancements in the area of novel electrochemical applications and industrial

applications.

Experimental

Preparation of Ni and Ni-ITO nanocomposite electrode

All chemicals were of analytical grade and the plating solutions were prepared in

double distilled water. Bath composition and operating conditions are shown in Table 1. The

required amount of ITO nanoparticles was mixed with nickel sulphamate bath solution and

agitated by a mechanical stirrer continuously for 8 h to achieve a homogeneous suspension.

An electrolytic grade pure nickel was used as the anode, mild steel specimen with an area of

2.5 cm × 5 cm was used as the cathode. The steel substrate was polished sequentially with 4,

5 and 6 grade emery papers and degreased with trichloroethylene and then electro-cleaned at

6 A dm^{-2} in 25 g l^{-1} Na$_2$CO$_3$ and 35 g l^{-1} NaOH solution at 70 $^{\circ}$C followed by activation in

5% H$_2$SO$_4$ solution for 20 seconds. A micro star pulse power supply (DPR 20-10-30, USA)

was used in the experiment for deposition of Ni and Ni-ITO nanocomposite coatings by pulse

currents.

Characterization of Ni and Ni-ITO nanocomposite electrode

Field emission scanning electron microscopy (FE-SEM) Carl Zesis and energy

dispersive X-ray spectrometer (Hitachi, Model S-3000H) were used to analyze the

morphological features and chemical composition of the Ni and Ni-ITO nanocomposite

deposits. Atomic Force Microscopy (AFM), Model Pico Scan 2100 (Molecular Imaging, USA) was employed in a contact mode with a silicon nitride tip to reveal the 3D surface topography of the deposits. X-ray diffraction patterns were recorded using a Bruker D8 Advance X-ray diffractometer with a Cu Kα radiation (λ = 1.5418˚A) and scanned at 10-100˚ (2θ) at a rate of 2 degree per minute. The wettability and water contact angle of deposited Ni and Ni-ITO nanocomposite were measured on Automatic Video based Contact angle measuring instrument from Data Physics Instruments GmbH (Model OCA 35, Germany). The analyses of Contact angle were carried out in static contact angle mode using Laplace-Young calculation method and the size of the water droplet was 5 μL for all the measurements.

Electro-reduction of nitrobenzene on Ni and Ni-ITO nanocomposite electrodes

Electrochemical measurements were performed on an Autolab PGSTAT-30 potentiostat/galvanostat (Eco Chemie, Netherlands) in a conventional three-electrode glass cell with an area of 1 cm^2 of the deposited Ni and Ni-ITO nanocomposite exposed on one side as working electrode, a platinum foil as counter electrode and an Ag/AgCl as reference electrode at 25 ± 1 °C.

Results and discussion

The chemical composition and weight percentage (Wt.%) of elements present in Ni-ITO nanocomposites were determined by the EDAX analysis as shown in Fig. 1(a-d), which clearly indicates the incorporation of the ITO nanoparticles in the Ni-ITO nanocomposite. The weight percentage of In and Sn in the nanocomposite is given in Table 2. The effect of concentration ITO nanoparticles in the electrolyte on weight percentage of ITO nanoparticles in the Ni-ITO nanocomposite is shown in Fig. 1e which is confirmed by EDAX analysis. It clearly reveals that the weight percentage nanoparticles in the nanocomposite depend on the concentration of suspended nanoparticles in the electrolyte. The weight percentage ITO

nanoparticles in the nanocomposite increases with the increasing concentration of the ITO nanoparticles and reaches the optimized incorporation of 1.74 wt.% at 2.5 g l^{-1}. Further increase in concentration of ITO nanoparticles above 2.5 g l^{-1} resulted a decrease in the weight percentage of ITO nanoparticles in the nanocomposite deposition as shown in Figs. 1(d and e). This indicated that the adsorption of ITO nanoparticles in the nanocomposites has reached the saturated state. According to Guglielmi's two-step adsorption mechanism,[31] the incorporation of ITO nanoparticles can be attributed to the adsorption of suspended particles on the cathode surface. Once particle is adsorbed, the metal starts build around the cathode slowly and incorporates the particles. As suggested by absorbing theory, the co-deposition of nanoparticles and metals on the cathode surface is through Vander walls forces.[32]

Figure 2 shows the FE-SEM images of the pulse electrodeposited Ni (hydrophobic) and Ni-ITO nanocomposite (super-hydrophobic) from nickel sulphamate electrolyte at 4 A dm^{-2} on mild steel substrate. As can be seen, nickel deposit revealed a pine-cone structure as shown in Fig 2a. Whereas, Ni-ITO nanocomposite in Fig. 2b clearly shows that, the pine-cone structure was modified into spherical structure due to the distribution of ITO nanoparticles reinforcements on the boundaries of nickel grains. These results suggest that surface featured with pine-cone (Ni) and spherical (Ni-ITO) micro-nano structure favours for acquiring the hydrophobic and superhydrophobic surfaces.

The wetting behaviour and water contact angle (CA) of the Ni and Ni-ITO nanocomposite at different concentration of ITO nanoparticles were measured. As shown in Fig. 3a pine-cone structure of Ni shows the contact angle is 110.5°. It indicates that the smooth surface of nickel can be turned up to hydrophobicity. The super-hydrophobic properties can be achieved either by (i) special surface chemistry (ii) surface geometrical microstructure (iii) enhancing surface roughness of hydrophobic materials and (iv) chemically modifying the micro-nano structure surface.[33] Therefore, nickel deposit required

one of the above critical conditions for the modification of the hydrophobic into superhydrophobic. However, after addition of ITO nanoparticles in the electrolyte, the contact angle is increased to 117°, 157.9 and 161.8 for 0.10, 0.56 and 1.74 wt.% of ITO nanoparticles in the nanocomposite. Furthermore, increasing the wt.% of ITO nanoparticles in the nanocomposites, increased contact angle and attains the optimum value of 161.8° at Ni-2.5 g l^{-1} ITO as shown in Fig. 3 (b-d). These results indicated that the Ni-ITO nanocomposite with spherical structure shows super-hydrophobic with high contact angle and possesses excellent water-repellent property than that of the pine-cone structure of nickel deposit. According to Wenzel's equation, the roughness is directly proportional to contact angle and inversely proportional to wettability as shown in the equation (1).[34]

$$\cos \theta = r \cos \theta_0 \qquad \qquad (1)$$

Where θ represents the apparent contact angle of water on the actual surface, θ_0 is the equilibrium contact angle on a smooth flat surface and r is the surface roughness ratio. Moreover, the addition of the ITO nanoparticles can generate numerous grooves on the nickel surface in which the air can be trapped and preventing the penetration of liquid droplets into the surface roughness that leads to the larger contact angle as proposed by Cassie-Baxter equation (2).[35]

$$\cos \theta = f_s \cos\theta_0 - (1-f_s) \qquad \qquad (2)$$

Where θ represents CA of water on a rough surface, θ_0 is the intrinsic contact angle on a flat surface. f_s and $(1-f_s)$ are the area fraction of solid surface and air. Therefore, it can be concluded that pine-cone structure of Ni deposit is naturally hydrophobic and modified the spherical structure with super-hydrophobicity due to the incorporation of ITO nanoparticles on the nickel deposit surface.

The surface roughness of nickel and Ni-ITO nanocomposites were characterized by Atomic Force Microscopy (AFM) are shown in Fig. 4. The average roughness (Ra) values are 0.08 μm and 0.22 μm for nickel and Ni-ITO nanocomposites. It was found that roughness increased with the addition of ITO nanoparticles compared with Ni. The higher roughness value contributes to the enhancement of the contact angle.[27] It was noted that the water droplets were unstable, anti-adhesive and immeasurable for Ni-ITO nanocomposites (CA 161.8 ˚).

The crystal phase and structure information of deposited Ni and different weight percentage of ITO nanoparticles with nickel nanocomposite were characterized by XRD analysis is shown in Fig. 5. It revealed that the diffraction peaks at 44.8˚, 52.2˚, 76.7˚, 93.2˚ and 98.7 were indexed as (111), (200), (220), (311) and (222) plane for face-centred cubic (fcc) of nickel (JCPDS Card No. 01-087-0712). The XRD pattern of the nanocomposite additionally shows small peak at 31˚for ITO nanoparticles as shown in Fig. 5d, indicating the presence of ITO in it. For Ni and Ni-ITO nanocomposite, the relative intensity of orientation is (200) and (111) respectively. Furthermore, the weight percentage of the ITO nanoparticles increasing with increased relative intensity of (111), (220), (311) and (222) planes compared with nickel. Qu et al., has reported a similar pattern for fabrication of Ni-CeO$_2$ nanocomposite.[36] It is because, with increase the concentration of ITO nanoparticles in the sulphamate bath, the growth of (200) orientation is inhibited as the formation of both hydrogen and nickel hydroxide are partially adsorbed on to the cathode surface during the electrodeposition of nickel that leads to the preferred relative intensity of (111) orientation for Ni-2.5 g l^{-1} ITO nanocomposite and suppresses the (200) orientation for Ni.

The super-hydrophobic Ni-ITO nanocomposite electrode was examined for the electrochemical catalytic activity. Electro-reduction of nitrobenzene was taken as a model reaction system. Fig. 6 shows the cyclic voltammograms of the reduction of nitrobenzene for

hydrophobic Ni (CA 110.5˚) and super-hydrophobic Ni-ITO nanocomposite (CA 161.8˚) electrode in pH 7 B-R buffer solution containing 3 mM nitrobenzene at 80 mVs^{-1}. The curve (blue) represents the smooth background voltammograms recorded for Ni electrode in buffer solution. The on-set potential for hydrogen evolution is around -750 mV. The hydrogen evolution potential shifted cathodically i.e., from -750 mV to -950 mV in the presence of nitrobenzene (curve black). No separate reduction peak/wave was observed for nitrobenzene on hydrophobic Ni (CA 110.5˚) electrode. The reduction of nitrobenzene merges with the hydrogen evolution process. On the other hand, a well distinct reduction peak at -950 mV was observed for nitrobenzene reduction process on the super-hydrophobic Ni-ITO nanocomposite electrode (CA 161.8˚) and no peak was observed in the reverse direction. The hydrogen evolution starts at -1.150 V. The reduction of nitrobenzene on super-hydrophobic Ni-ITO nanocomposite (CA 161.8˚) electrode takes place at lesser potential with appreciable/measurable current compared to hydrophobic Ni (CA 110.5˚) electrode. The electrocatalytic behaviour of nitrobenzene reduction process is attributed to higher active surface area of super-hydrophobic Ni-ITO nanocomposite electrode. The cyclicvoltammetric studies revealed the scope for further investigation on the reduction nitrobenzene and other organic molecules.

Conclusions

In this work, we presented the low-cost and facile method of pulse electrodeposition for preparation of super-hydrophobic Ni-ITO nanocomposite without crystal modification and showed the electrochemical activities for reduction of nitrobenzene. The as-prepared Ni and Ni-ITO nanocomposite electrodes were characterized by EDAX, FE-SEM, AFM, XRD and contact angle measurements. It was found that with the incorporation of ITO nanoparticles, the morphology of the nickel deposit changed from pine-cone to spherical structure. The weight % of ITO nanoparticles in the deposit increases with increasing ITO nano particles

concentration in the electrolyte. With the addition of ITO nanoparticles, the relative intensities of (111), (220), (311) and (222) orientation significantly increased compared with (200) orientation of pure nickel. The water contact angle of the nickel deposit varied from 110˚ (hydrophobic) to 161.8˚ (super-hydrophobic) with the addition of ITO nanoparticles. Cyclic voltammetry result showed that, Ni-ITO nanocomposite electrode increases the electrocatalytic activity towards electro-reduction of nitrobenzene compared with pure Ni.

Notes and references

1. T. Liu, Y. Yin, S. Chen, X. Chang and S. Cheng, Electrochim. Acta., 2007, **52,** 3709.

2. Y. Wang, W. Wang, L. Zhong, J. Wang, Q. Jiang and X. Guo, Appl. Surf. Sci., 2010, **256,** 3837.

3. W. Zhang, Z. Yu, Z. Chen and M. Li, Mater. Lett., 2012, **67,** 327.

4. W. Xu, X. Shi and S. Lu, Mater. Chem. Phys., 2011, **129,** 1042.

5. Z. Chen, F. Tian, A. Hu and M. Li, Surf. Coat. Technol., 2013, **231,** 88.

6. Z. Chen, L. Hao, A. Chen, Q. Song and C. Chen, Electrochim. Acta., 2012, **59,** 168.

7. S. Kulinich, S. Farhadi, K. Nose and X. Du, Langmuir., 2010, **27,** 25.

8. L.J. Chen, M. Chen, H.D. Zhou and J.M. Chen, Appl. Surf. Sci., 2008, **255,** 3459.

9. J. Bico, C. Marzolin and D. Que´re´, Eur. Phys. Lett., 1999, **47,** 220.

10. L. Feng, S. Li and Y. Li, Adv. Mater., 2002, **14,** 1857.

11. O.U. Nimittrakoolchai and S. Supothina, J. Eur. Ceram. Soc., 2008, **28,** 947.

12. F. Zhang, S. Chen, L. Dong, Y. Lei, T. Liu and Y. Yin, Appl. Surf. Sci., 2011, **257,** 2587.

13. Z. She, Q. Li, Z. Wang, L. Li, F. Chen and J. Zhou, Chem. Eng. J., 2013, **228,** 415.

14. P. Wang, D. Zhang and R. Qiu, Corros. Sci., 2012, **54,** 77.

15. A. Satyaprasad, V. Jain and S.K. Nema, Appl. Surf. Sci., 2007, **253,** 5462.

16. H. Liu, L. Feng, J. Zhai, L. Jiang and D. Zhu, Langmuir., 2004, **20,** 5659.

17. R. Yang, A. Asatekin and K.K. Gleason, Soft Matter., 2012, **8,** 31.

18. R.V. Lakshmi, T. Bharathidasan, P. Bera and B.J. Basu, Surf. Coat. Technol., 2012, **206,** 3888.

19. N.A. Ahmad, C.P. Leo and A.L. Ahmad, Appl. Surf. Sci., 2013, **284,** 556.

20. Y. Fan, C. Li, Z. Chen and H. Chen, Appl.Surf. Sci., 2012, **258,** 6531.

21. A. Nakajima, K. Abe, K. Hashimoto and T. Watanabe, Thin Solid Films., 2000, **376,** 140.

22. Y. Li and G. Q. Shi, J. Phys. Chem. B., 2005, **109,** 23787.

23. Yunhuai Zhang, Yannan Yang, Peng Xiao, Xiaoning Zhang and Lu Li, Mater. Lett., 2009, **63,** 2429.

24. Hui Zhang, Jing-Juan Xu and Hong-Yuan Chen, J. Phys. Chem. C., 2008, **112,** 13886.

25. Jie Liu, Cheng Zhong, Xintong Du, Yating Wu, Peizhi Xu, Jinbo Liu and Wenbin Hu, Electrochim. Acta., 2013,**100,** 164.

26. Kuo-Chiang Lin, Yu-Ching Lin and Shen-Ming Chen, Electrochimica Acta., 2013, **96,** 164.

27. S. Khorsand, K. Raeissi and F. Ashrafizadeh, Appl.Surf. Sci., 2014, **305,** 498.

28. Tao Hang, Anmin Hu, Huiqin Ling, Ming Li, Dali Mao, Appl.Surf. Sci., 2010, **256,** 2400.

29. J. Liu, C. Zhong, X. Du, Y. Wu, P. Xu, J. Liu and W. Hu, Electrochim. Acta., 2013, **100,** 164.

30. Hoo Keun Park, Seong Woong Yoon, Won Woo Chung, Byoung Koun Minb and Young Rag Do, J. Mater. Chem. A., 2013, **1,** 5860.

31. N. Guglielmi, J. Electrochem. Soc., 1972, **119,** 1009.

32. R. Xu, J. Wang, L. He and Z. Guo , Surf. Coat. Technol., 2008, **202,** 1574.

33. R. Fürstner, W. Barthlott, C. Neinhuis and P. Walzel, Langmuir, 2005, **21,** 956.

34. S. Kulinich and M. Farzaneh, Langmuir, 2009, **25,** 8854.

35. R.N. Wenzel, J. Phys. Chem., 1949, **53,** 1466.

36. N.S. Qu, D. Zhu and K.C. Chan, Scripta Mater., 2006, **54,** 1421.
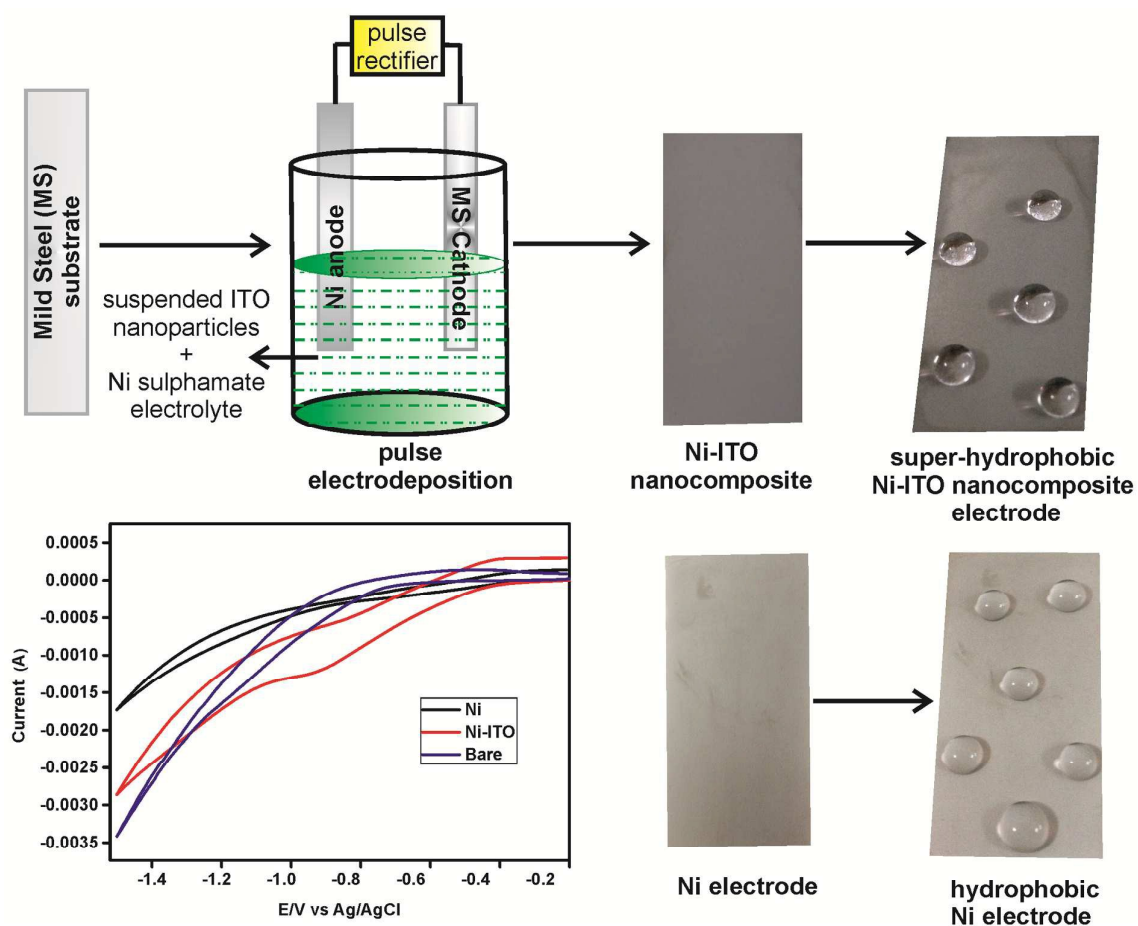
Scheme 1 Schematic illustration of the preparation of pulse electrodeposited super-hydrophobic Ni-ITO nanocomposite for electro-reduction of nitrobenzene.
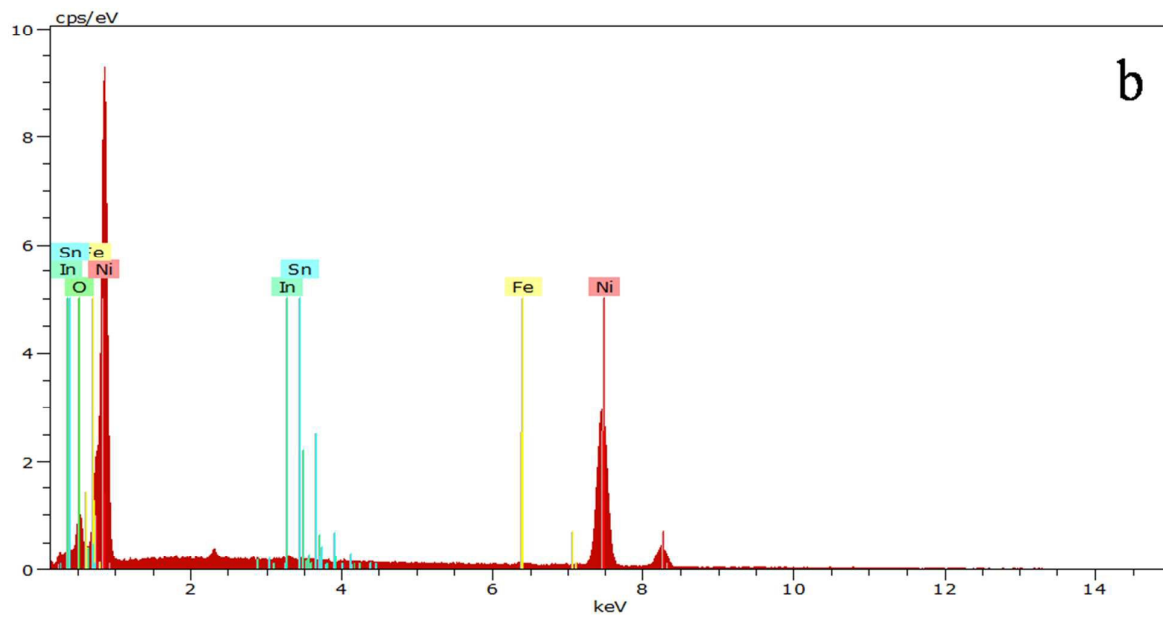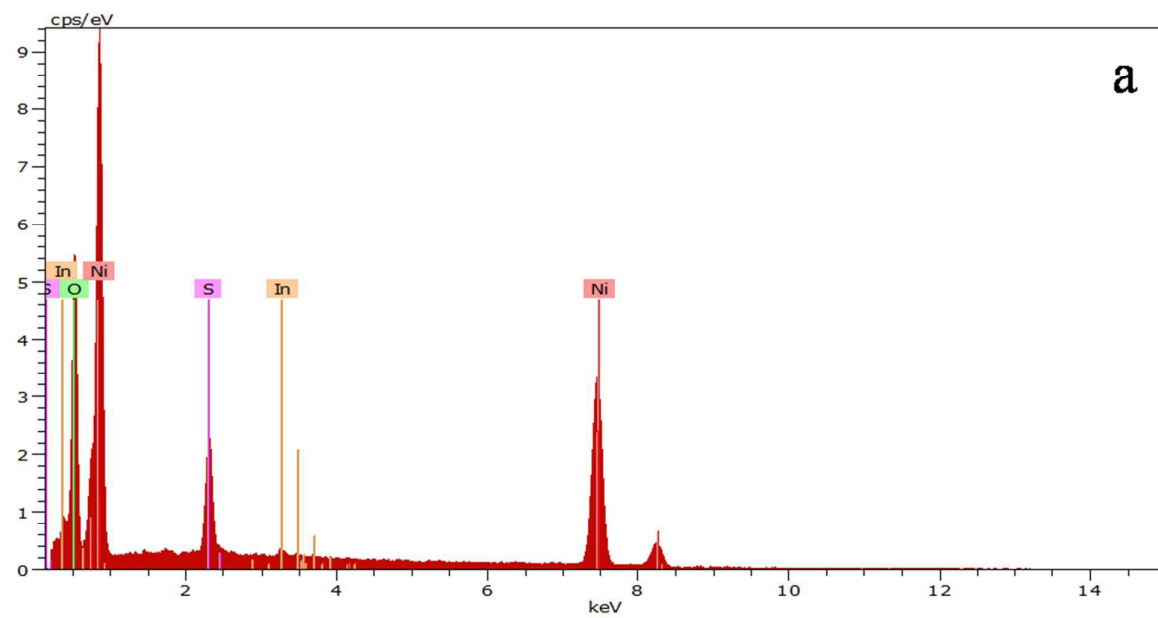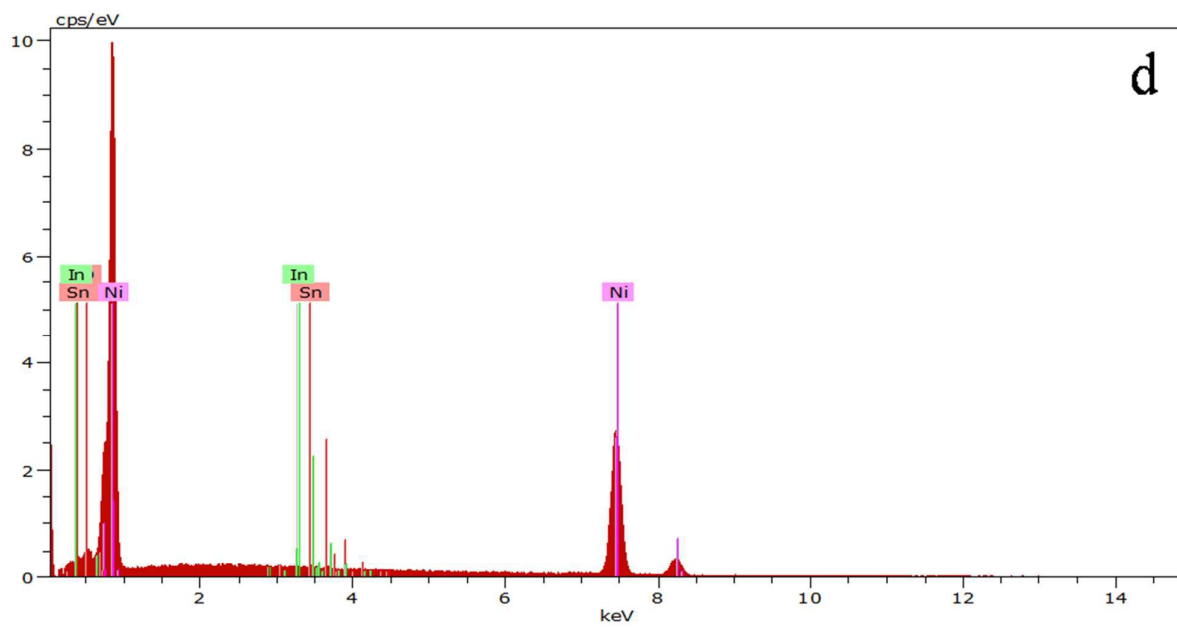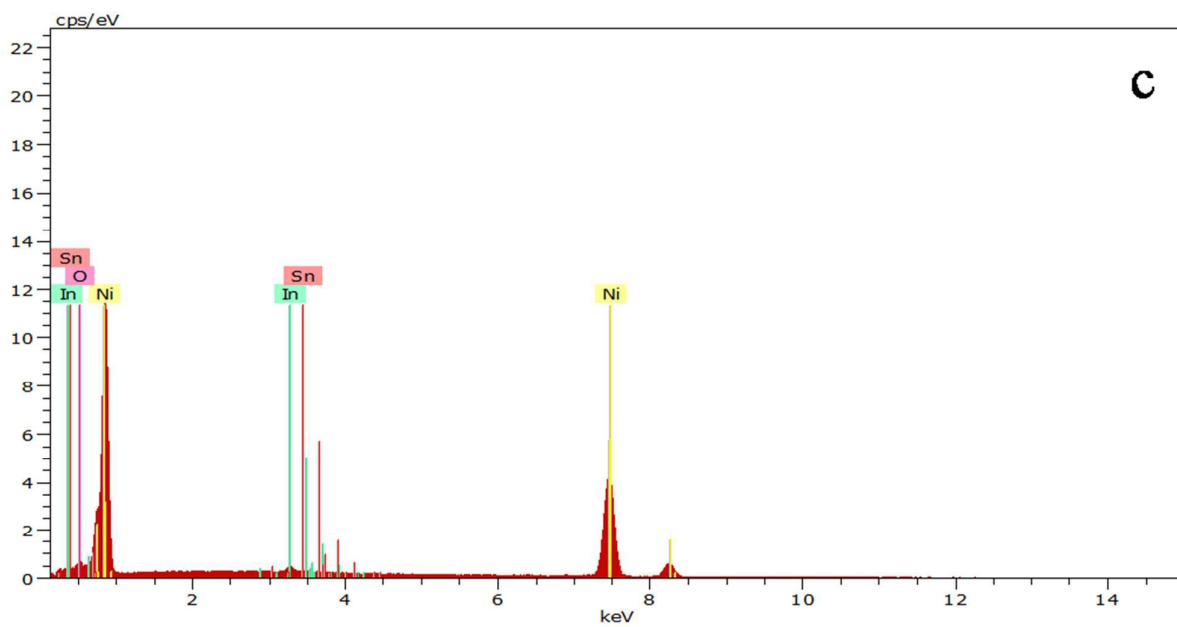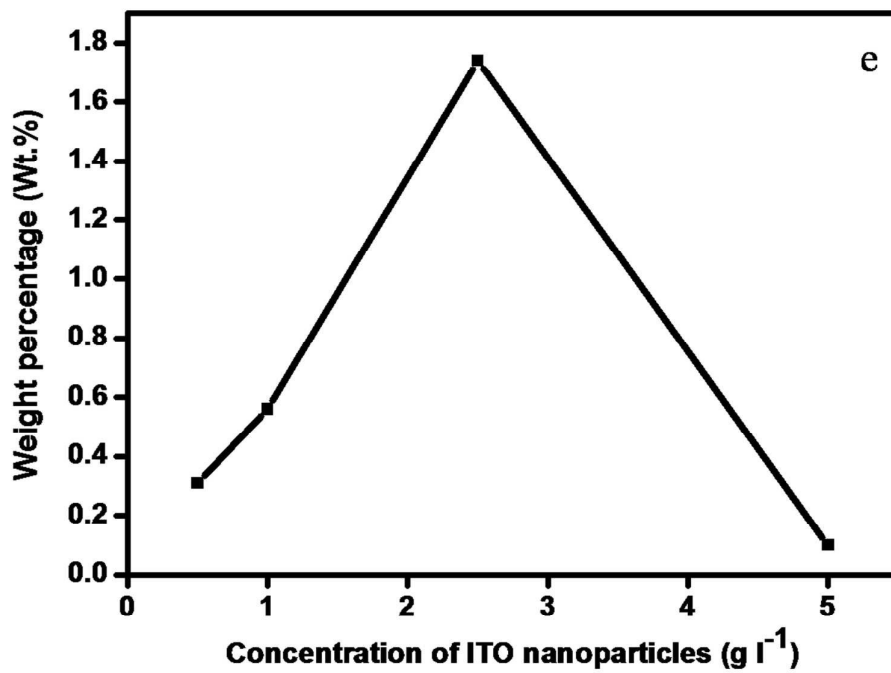
Fig. 1 EDAX analysis of (a) Ni-0.5 g l^{-1} ITO (b) Ni-1 g l^{-1} ITO (c) Ni-2.5 g l^{-1} ITO (d) Ni-5 g l^{-1} ITO nanocomposite and (e) effect of ITO nanoparticles in the electrolyte on weight percentage of ITO nanoparticles in the Ni-ITO nanocomposite.
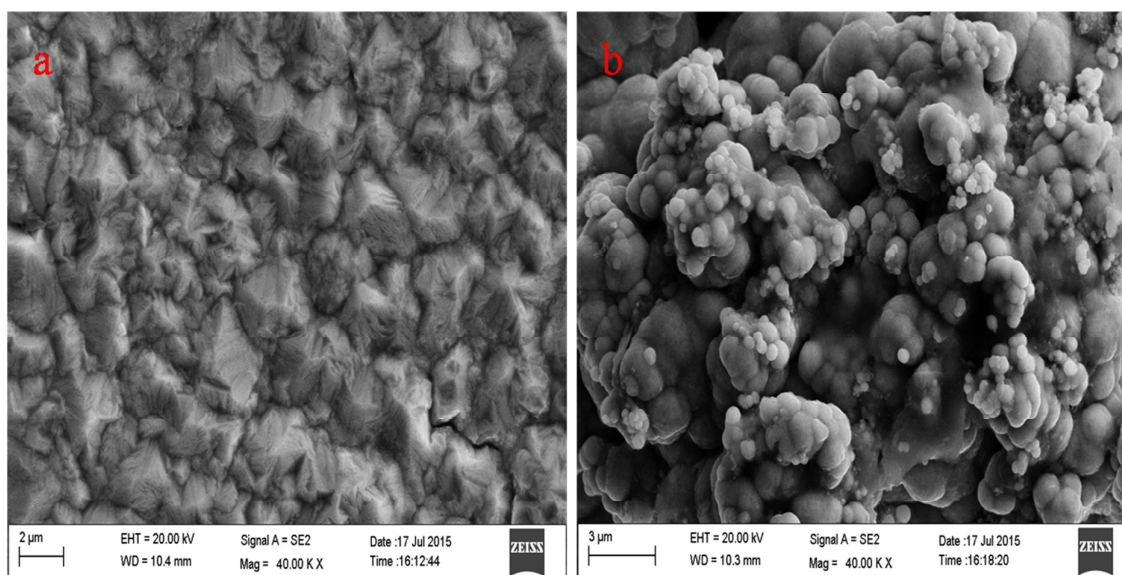
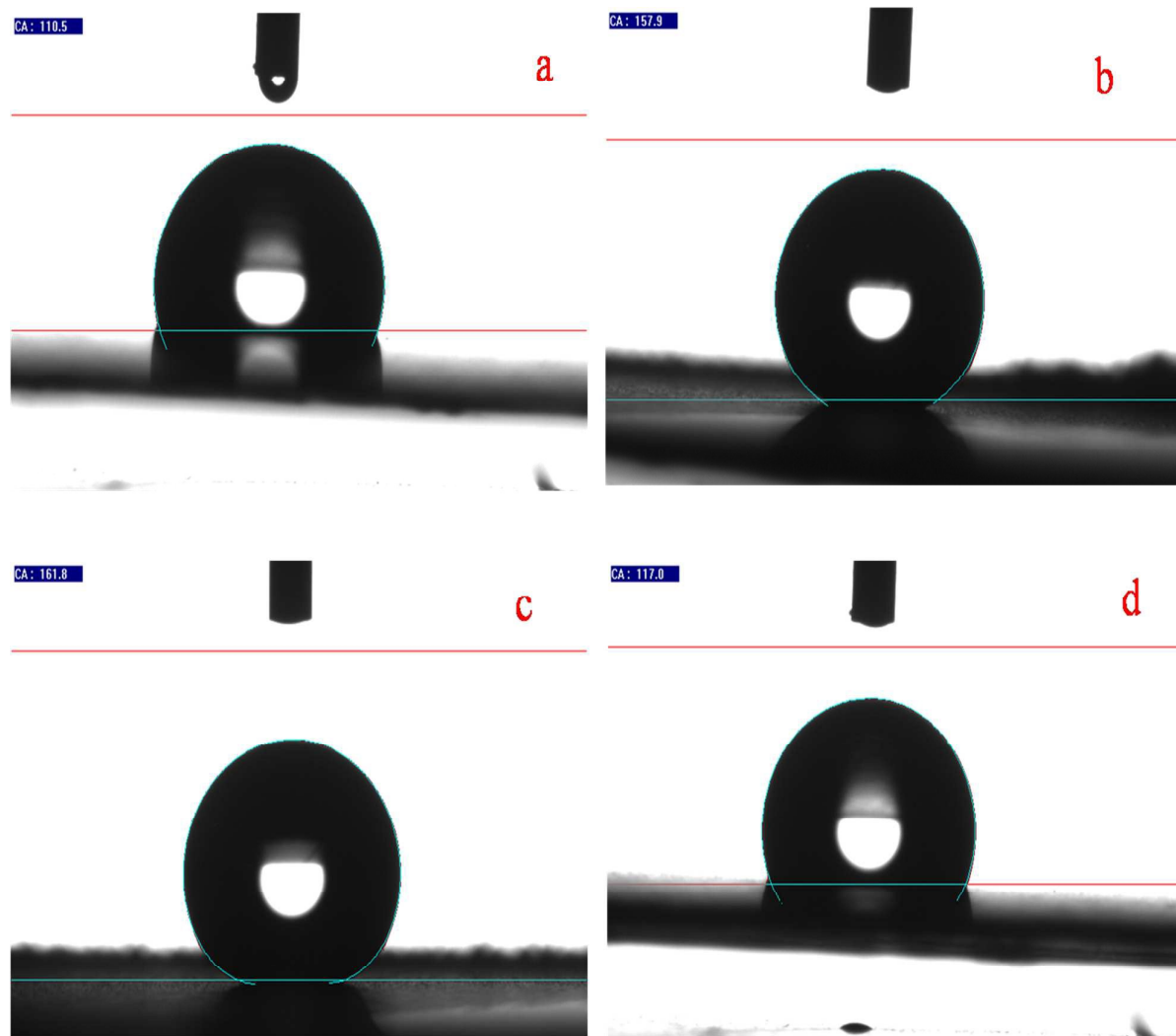**Fig. 2** FE-SEM images of (a) Ni and (b) Ni-2.5 g l^{-1} ITO nanocomposite.

Fig. 3 Water contact angle measurements on (a) Ni (b) Ni- 0.56 wt.% ITO (c) Ni-1.74 wt.%
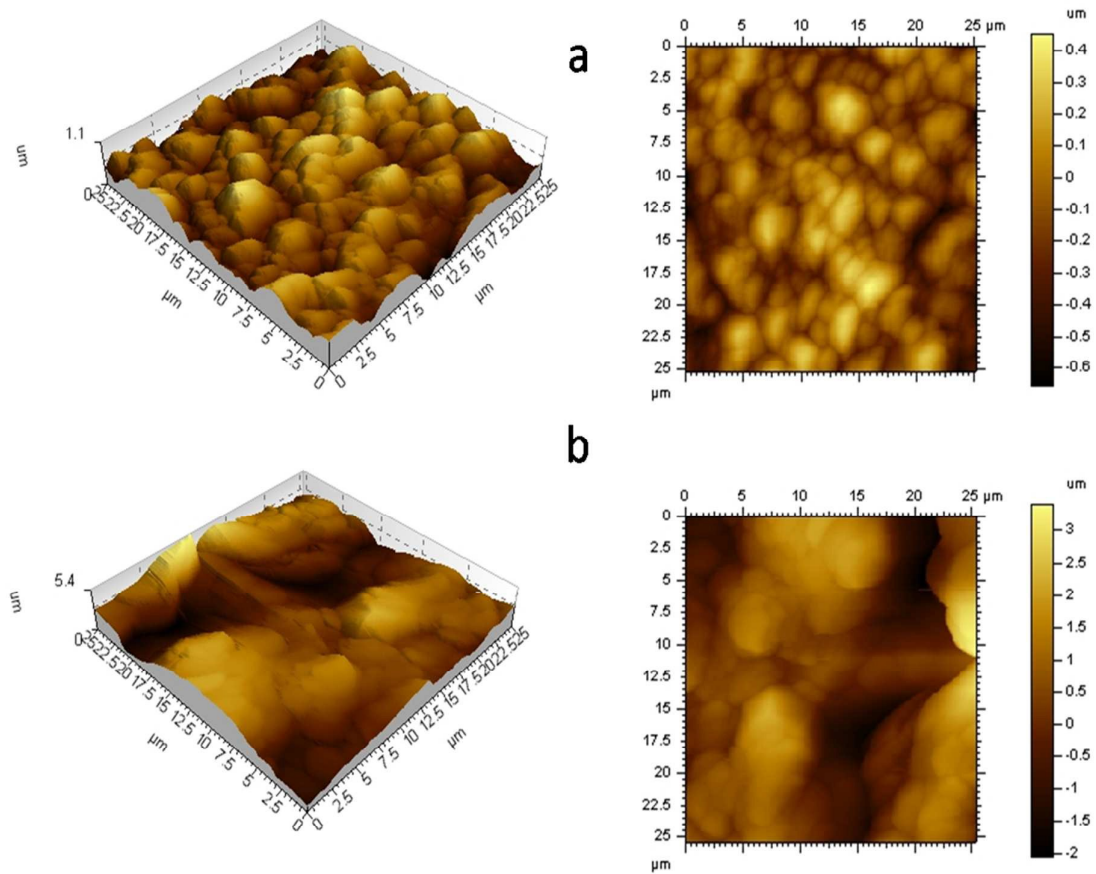
ITO and (d) Ni-0.10 wt.% ITO nanocomposite.

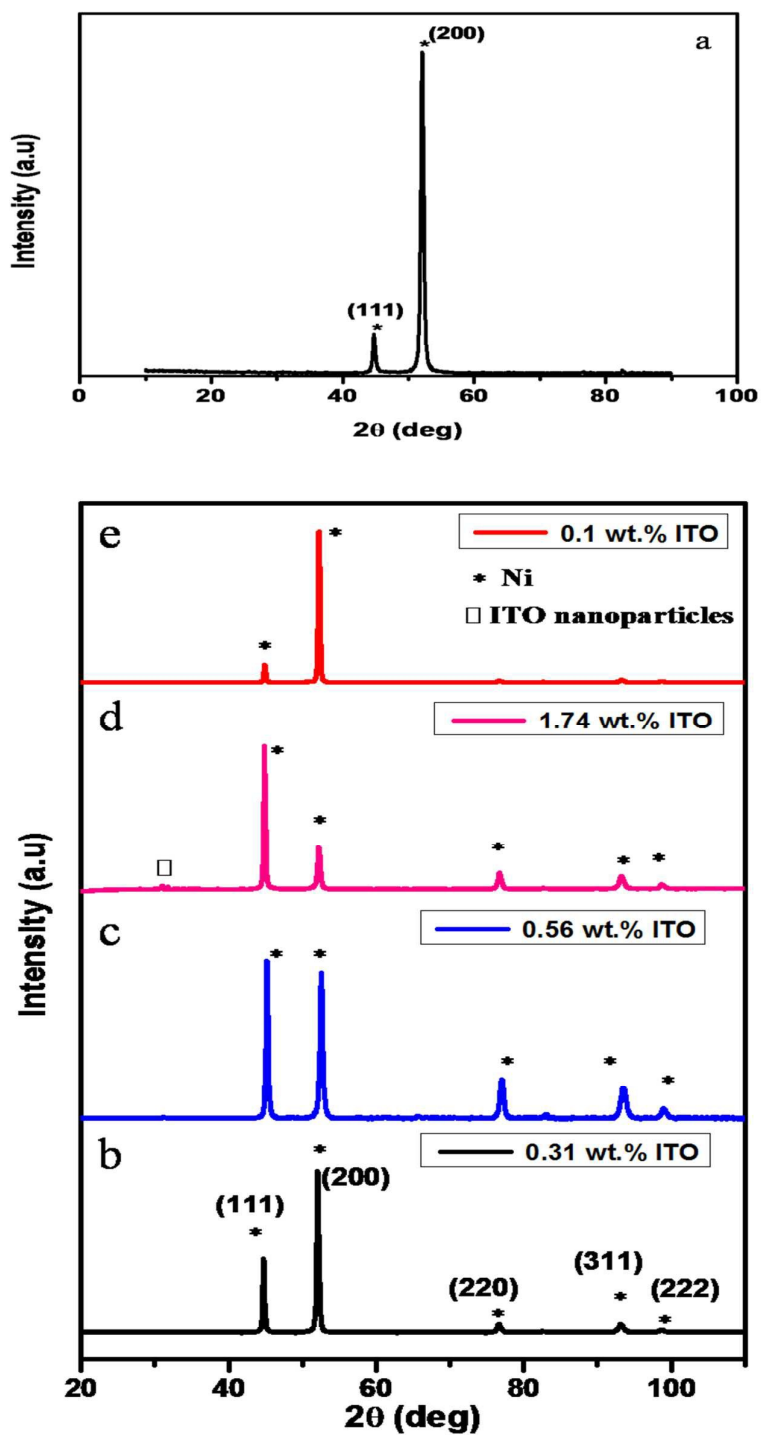**Fig. 4** AFM images of (a) Ni and b) Ni-2.5 g l^{-1}ITO nanocomposite.

Fig. 5 Typical XRD pattern of (a) Ni (b) Ni-0.31 wt.% ITO (c) Ni- 0.56 wt.% ITO (d) Ni-1.74 wt.% ITO and (e) Ni-0.10 wt.% ITO nanocomposite.
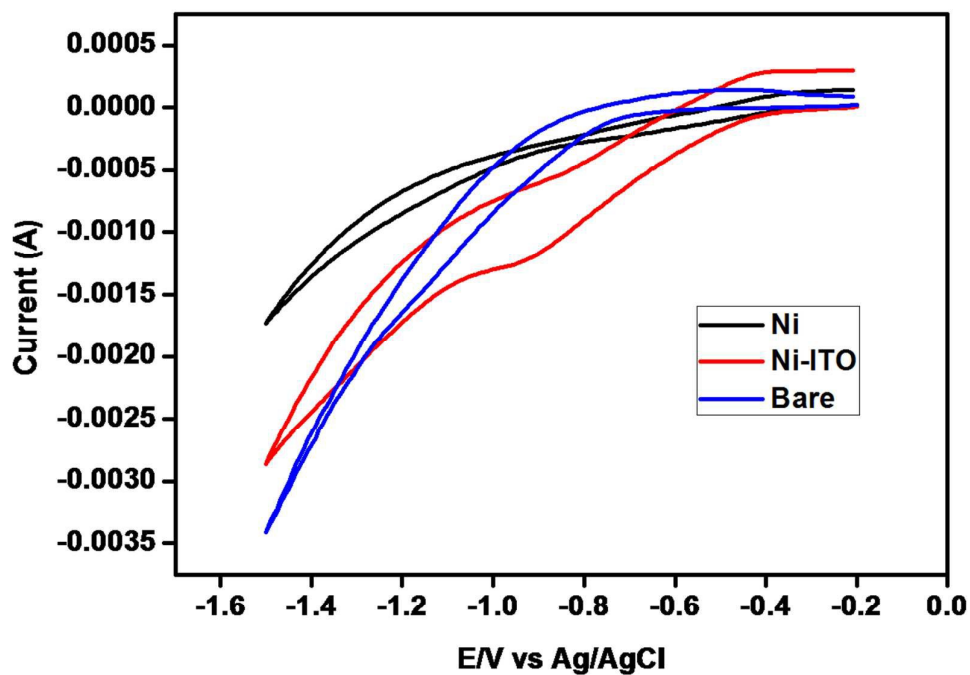
Fig. 6 Cyclic voltammograms of Ni (hydrophobic) and Ni-ITO nanocomposite (super-hydrophobic) electrode for electro-reduction of nitrobenzene in pH 7 B-R buffer solution containing 3 mM nitrobenzene at 80 mVs^{-1}.

Table 1 Bath composition and operating conditions of nickel sulphamate plating bath.

Bath constituents	Composition and operating conditions
$Ni(SO_3NH_2)_2$ (Nice Chemicals)	300 g l^{-1}
H_3BO_3 (Nice Chemicals)	40 g l^{-1}
$NiCl_2 \cdot 6H_2O$ (Nice Chemicals)	5 g l^{-1}
Sodium lauryl sulphate (Nice Chemicals)	0.05 g l^{-1}
ITO nanoparticles (Sigma Aldrich)	0.5, 1, 2.5 and 5 g l^{-1}
Current density	4 A dm^{-2}
pH	3
Time	30 min
Temperature	50 ∘C
Stirring	600 rpm
Pulse duty cycle	10%
Pulse frequency	10 Hz

Table 2 Effect of ITO nanoparticles in the electrolyte on weight percentage of ITO nanoparticles in the Ni-ITO nanocomposite.

Concentration of ITO nanoparticles in nickel sulphamate electrolyte (g l^{-1})	Weight percentage of In and Sn nanoparticles in Ni-ITO nanocomposite (wt.%)
0.5	0.31
1	0.56
2.5	1.74
5	0.10